# Adapting Biomimetic Kinematics for Controlling a Powered-Knee, Passive-Ankle Prosthesis Across Inclines

C. Andrew Seelhoff[1], T. Kevin Best[2] , and Robert D. Gregg[1,2]

***Abstract*— Despite promising benefits for people with limb loss, powered multi-joint prostheses from the research field have not been translated into the clinical space. Commercial powered knee prostheses like the Össur Power Knee™ are paired with passive feet which lack the range of motion of biological ankle joints, especially on steep inclines. This discrepancy prevents the direct translation of emerging biomimetic control methods for powered knee-ankle prostheses, which implicitly assume both joints exhibit normative biomechanics. To enable commercial prostheses to benefit from biomimetic control methods on inclines, this paper adapts a continuous knee kinematic model to minimize the difference in global foot angle compared to able-bodied reference data, under the assumption that the ankle joint is locked. In a pilot experiment with an above-knee amputee participant, our adapted controller produced substantial benefits compared to a baseline controller that only tracks able-bodied knee trajectories. Level-ground walking performance is similar to existing methods despite the change of objective, and on steep inclines, prosthesis load-bearing and center of pressure progression are restored to near-normative levels. These results show a promising pathway towards translation of biomimetic control methods onto existing commercial hardware, allowing near-term impacts with tangible benefits for prosthesis users.**

## I. Introduction

There are over two million people with limb loss in the United States [1], and this population is expected grow a further 150% by 2060 [2]. The limb loss population experiences reduced quality of life as most current prosthetic limbs are unable to replicate the joint torques normally provided by intact musculature, resulting in an increased metabolic cost of walking [3], [4]. Activities which require net-positive work, such as walking up ramps or stairs, further exacerbate these deficiencies. In response, the research field has made substantial progress developing multi-joint powered prostheses, which place motors at the knee and ankle joint to allow the limb to propel itself and assist the user during ambulation [5], leading to reductions in metabolic cost, increasing walking speed, and even reducing compensatory behaviors [6]–[8].

There has been limited, but growing, commercial development of powered prostheses, including one powered ankle, the Empower (Otto Bock, Duderstadt, Germany), and three powered knee prostheses: the Power Knee™ (Össur hf, Reykjavík, Iceland), the Intuy Knee (Reboocon, Delft, The Netherlands), and the Bio Leg (BionicM, Tokyo, Japan). The primary obstacles towards clinical adoption of powered prostheses are their bulkiness and complexity compared to existing passive solutions [5]. While commercial powered knees are typically heavier than passive counterparts, they occupy a similar form factor. Powered ankles, however, are much heavier and larger than passive Energy Storage and Return (ESR) feet, which consist of fiberglass or carbon fiber springs. Combining powered joints also presents a complex, interdependent control problem, often involving dozens of user-specific parameters [9]. As a result, commercially-available powered transfemoral prostheses primarily use a *powered-knee, passive-ankle* configuration to minimize distal mass and reduce complexity.

Although ESR feet lack a physical joint, they can emulate a limited ankle range of motion (RoM) through deformation of the elastic heel and keel. ESR feet are designed primarily to facilitate level walking, where able-bodied RoM is relatively limited [10], but in other activities, the prosthesis-side gait kinematics depart substantially from able-bodied data [11], [12]. As a result, prosthesis users experience reduced symmetry and stability [13], [14] and must make gait compensations on inclines, [15], declines [16], and stairs [17]. Effective RoM can be marginally increased by making the ESR foot less stiff, although this comes at a cost of lower energy-return, leading to further physical and perceptual changes to gait [18]–[20].

Because of these limitations of ESR feet, powered knee, passive-ankle prostheses have not yet achieved the versatility of powered knee-ankle prostheses, which can facilitate variable-speed/incline walking [21]–[23], variable-height stair climbing [24], [25], and continuous transitions between these activities [26]. Many multi-joint controllers are designed to reproduce able-bodied joint trajectories to promote more normative gait while reducing (or eliminating) hand-tuned parameters [27]–[29]. Able-bodied joint patterns are typically parameterized by a phase variable, which can be calculated using residual-limb thigh kinematics to synchronize the prosthesis to the user's movement [21], [22], [30]. Our group initially implemented position controllers using continuous-phase/task models of able-bodied joint kinematics [31], [32], although shortcomings in resultant gait kinetics led to the use of data-driven joint impedance during the stance phase [22]. These hybrid kinematic impedance controllers improved joint work [22], [24], symmetry [33], and endurance measures [34] when implemented on a prototype powered knee-ankle prosthesis [35]. However, these biomimetic controllers cannot be directly translated onto

This work was supported by the National Institute of Child Health & Human Development of the NIH under Award R01HD094772, by the University of Michigan Rackham Merit Fellowship, and by the National Science Foundation under the Graduate Research Fellowship DGE 1841052. Hardware was provided by Össur hf (Reykjavík, Iceland).

[1]Department of Mechanical Engineering, [2]Department of Robotics, University of Michigan, Ann Arbor, MI 48109, USA. Contact: {seelhoff, tkbest, rdgregg}@umich.edu

powered-knee, passive-ankle prostheses, as they implicitly expect biological ankle behavior which ESR feet cannot provide on uneven terrains. To have tangible short-term impact, we must adapt multi-joint prosthesis control methods for use with powered-knee, passive-ankle prostheses, especially for inclined walking.

In this work, we introduce a novel knee prosthesis controller designed to account for ESR foot behavior on inclines. As a proof-of-concept, we alter the knee kinematic model of a PD position controller by simulating the effects of an ESR foot on able-bodied foot kinematics. We describe the optimization process for generating continuous knee trajectories as a function of gait phase, walking speed, and incline, focusing on achieving more biomimetic foot angle kinematics in place of biomimetic knee angle kinematics. Pilot experiments with one transfemoral amputee subject suggest the proposed *ESR-Adapted* controller greatly mitigates gait alterations imposed by ESR feet on steep inclines without sacrificing level-ground performance when compared to a biomimetic kinematic control strategy. The results demonstrate the potential for our controller to be further refined and adapted to other gait tasks, improving mobility for users of powered-knee, passive-ankle prostheses and making the case for more widespread adoption of powered prostheses.

## II. Methodology

### A. Hardware Overview

In this study, we utilize the latest generation Power Knee from Össur (model PKA01). The drivetrain of the Power Knee consists of a brushless DC motor, a harmonic drive transmission, and a compliant linkage that connects the transmission output to the knee joint. The torque-angle relationship of the compliant linkage is nonlinear, stiffening under increasing deflection. The knee assembly weighs 2.7 kg with the battery, and the joint has a 120 deg RoM. The removable lithium ion battery powers the motor and the embedded control electronics.

The sensing suite includes joint and motor position encoders, a shank-mounted inertial measurement unit, and an array of ground reaction force hall-effect sensors [36]. Based on the manufacturer's recommendations, we paired the Power Knee with the Össur Pro-Flex LP carbon fiber ankle-foot prosthesis. We selected the appropriate size and category foot (size R28 category 5) for our participant based on the sizing guidelines in the Pro-Flex LP catalog. The entire prosthesis, including the Power Knee, pylon, foot, shoe, and other hardware components configured for our participant, weighed 3.9 kg.

### B. Controller Overview

Previous work in our group has shown success with continuous parametrization of joint angles in walking as a function of gait phase, incline, and speed [31], [32]. We adapted this control architecture for use on powered-knee, passive-ankle prostheses by removing the ankle dependency, yielding a singular position controller for the knee (Fig. 1). We constructed and tested two kinematic models for this

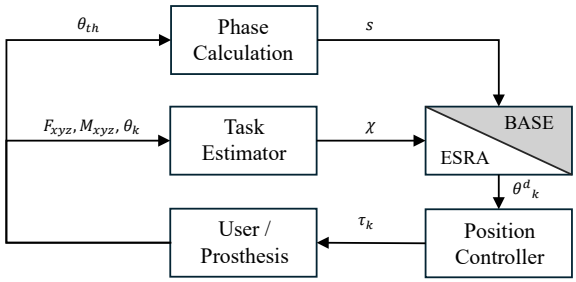


Fig. 1. Block diagram of the proposed control architecture, adapted from [32]. A phase estimate $s$ and task estimate $\chi$ feed into either the baseline model (BASE) or the ESR-Adapted model (ESRA). While the BASE model generates a knee trajectory based on able-bodied reference data, the ESRA model described in this work accounts for ESR behavior. Both models produce a desired knee angle $\theta_k^d$ which is sent to the PD Position controller, driving the prosthesis. Interactions between the user, prosthesis, and environment generate external forces and moments $F_{xyz}, M_{xyz}$ and alter the knee and thigh angles $\theta_k, \theta_{th}$.

controller. The *baseline* (BASE) model is similar to the model used in [31], [32], directly tracking biological knee kinematics assuming the ankle is also actuated within biological ranges of motion. The *ESR-Adapted* (ESRA) model was designed to account for ESR foot behavior.

Both models interfaced with the same PD position controller, which was parameterized by the gait phase $s$ and task vector $\chi = (v, \gamma)$, where $v$ represents the user's forward speed and $\gamma$ represents the ground slope. The PD controller commanded a torque $\tau_k$ and was defined as

$$\tau_k(s,\chi) = k_p e(s,\chi) + k_d \dot{e}(s,\chi), \tag{1}$$

where $e(s,\chi)$ represents the error in knee position $\theta_k(s,\chi)$ compared to a desired position $\theta_k^d(s,\chi)$, and $\dot{e}$ is its derivative. The proportional and derivative gains $k_p$ and $k_d$ were set to values previously used by our group for PD position control of a multi-joint powered prosthesis. The *task space* spanned forward speeds within $v \in [0.8, 1.2]$ m/s and slopes within $\gamma \in [0, 10]$ deg.

### C. Knee Kinematic Models

Following previous work from [31], we model the knee angle trajectory for a given task $\chi$ as a phase-dependent Fourier Series of degree $k$ with the following equation:

$$\theta_k(s,\chi) = \alpha_0(\chi) + \sum_{n=1}^{k} (\alpha_n(\chi)\sin(2\pi n s) + \beta_n(\chi)\cos(2\pi n s)), \tag{2}$$

where $s \in \{0,1\}$ and the weights $w(\chi) = (\alpha_0, ..., \alpha_k, \beta_1, ..., \beta_k) \in \mathbb{R}^{2k+1}$ are used as decision variables for optimization. Selecting the degree $k = 5$ enables the Fourier Series to successfully replicate able-bodied knee kinematic trajectories without overfitting. With all terms being periodic, the Fourier Series ensures there is continuity between the end of one stride and the start of the next. We can also write (2) as

$$\theta_k(s,\chi) = A(s,\chi) w(\chi), \tag{3}$$

where $w(\chi) = (\alpha_0, ..., \alpha_5, \beta_1, ..., \beta_5) \in \mathbb{R}^{11}$. The matrix $A \in \mathbb{R}^{1500\times11}$ contains 10 concatenated sets of the basis functions 1, $\sin(2\pi s)$, $\cos(2\pi s)$, ..., $\sin(10\pi s)$, $\cos(10\pi s)$ evaluated at 150 discrete values of phase $s$, linearly spaced between 0 and 1, for the given task $\chi$. Each $\mathbb{R}^{150\times11}$ set of basis functions corresponds to one of the $n = 10$ subjects in an able-bodied reference dataset collected by our group [37].

For both kinematic models, at each task, we aim to find the optimal weights $w_{\text{opt}}(\chi)$ to satisfy our control objective $J(s, \chi, w)$, which differs between the two models:

$$w_{\text{opt}}(s, \chi) = \arg\min_{w\in\mathbb{R}^{11}} J(s, \chi, w). \tag{4}$$

The specific objective functions and optimization methods used for each kinematic model are described below. For each model, we solve the optimization problem for a set of discrete tasks within our task space according to the able-bodied reference data from n = 10 subjects [37]. We include all available speeds ($v = \{0.8, 1.0, 1.2\}$ m/s) and all positive-slope inclines ($\gamma = \{0, +5, +10\}$ deg) from the dataset, resulting in $3 \times 3 = 9$ discrete tasks for evaluation. Then, using the fact that our function for $\theta_k$ is linear with respect to $w$, we perform bilinear interpolation in terms of speed and incline between these nine tasks to generate continuous kinematic surfaces.

*1) Baseline Kinematic Model:* The baseline kinematic model is created using the existing methodology in [31] for comparison with our proposed kinematic model. Our objective function is the error in knee trajectory:

$$J_{\text{BASE}}(s, \chi, w) = \|(A(s, \chi)w - \theta_k^{\text{ref}}(s, \chi)\|^2, \tag{5}$$

where $\theta_k^{\text{ref}}(s, \chi)$ is the able-bodied reference knee trajectory at phase $s$ and task $\chi$. Similar to $A$, the reference trajectories for each subject are concatenated vertically to allow for subject-average optimization. Substituting (5) into (4) yields a least-squares optimization problem with a known closed-form solution. Fig. 2 (left) shows the kinematic surface generated through optimization across all inclines at a fixed speed of 1 m/s.

*2) ESR-Adapted Kinematic Model:* Previous pilot testing revealed that our baseline kinematic model, which assumes the ESR foot behaves exactly as an able-bodied ankle, can result in unfavorable behaviors during activities with high ankle RoM. These shortcomings inform the design of a modified controller which accounts for ESR foot mechanics. This control method requires an objective function that allows the Power Knee to influence foot behavior while accounting for the ESR behavior itself.

First, we model the alterations to biological kinematics caused by an ESR foot. Setting the kinematic origin of the leg at the hip, forward kinematics define the position of each joint center progressing distally, ending with the (global) foot angle and position. An ideal model would simulate the deformation of the ESR foot through ground contact simulation, but the sheer variety of ESR feet in terms of stiffness, RoM, and size make this approach practically infeasible for generalization. As such, we elect to take the reduced RoM to its extreme, modeling the ankle as fixed at its neutral ankle, yielding the following equation for foot angle, defined with respect to the horizontal:

$$\theta_{\text{foot}}(s, \chi) = \theta_{\text{thigh}}^{\text{ref}} - \theta_k + \theta_{\text{ankle}}^{\text{f}} = \theta_{\text{thigh}}^{\text{ref}} - Aw, \tag{6}$$

where $\theta_{\text{thigh}}^{\text{ref}}$ is the reference global thigh angle angle from [37] with all ten subjects' trajectories concatenated vertically and $\theta_{\text{ankle}}^{\text{f}}$ is the fixed ankle angle, which is 0 deg with respect to vertical. All variables are dependent on the current phase $s$ and task $\chi$.

The ankle's rigidity results in an overly-plantarflexed foot throughout stance phase in simulation, which would result in improper loading on the keel of the prosthesis. A feasible optimization objective would be restoration of a biological foot angle trajectory through stance phase. Since there is no ground contact during swing phase, we use a biological knee angle tracking objective after toe-off to allow for biomimetic swing behavior. The first component of this modified objective function is

$$J_{\text{ESRA}}^1(s, \chi) = \begin{cases} \|\theta_{\text{foot}} - \theta_{\text{foot}}^{\text{ref}}\|^2 & \text{for } s \le s_{\text{TO}} \\ J_{\text{BASE}} & \text{otherwise} \end{cases} \tag{7}$$

with the toe-off threshold $s_{\text{TO}} = 0.64$ selected based on able-bodied reference data [37].

In preliminary testing, the foot angle objective alone caused rapid extension of the knee in early stance phase. To balance this behavior and make heel-strike and midstance smoother, we penalize the knee velocity $\dot{\theta}_k(s)$ during the first three-quarters of stance phase, giving the second objective component

$$J_{\text{ESRA}}^2(s, \chi) = \begin{cases} (4 - \frac{4s}{0.75 s_{\text{TO}}})\dot{\theta}_k(s)^2 & \text{for } s \le 0.75 s_{\text{TO}} \\ 0 & \text{otherwise} \end{cases} \tag{8}$$

where the coefficient on $\dot{\theta}_k(s)^2$ linearly decreases from 4 to 0 over the range $s \in [0, 0.75 s_{TO}]$. The knee velocity is given by

$$\dot{\theta}_k(s) = \frac{\partial A}{\partial s}\frac{\partial s}{\partial t}w, \tag{9}$$

where $\frac{\partial A}{\partial s}$ is the element-wise derivative of $A$ with respect to phase, and $\frac{\partial s}{\partial t} = 1$ as we assume each stride has a duration of one second.

Due to the linearity of $\theta_k$, $\theta_{\text{foot}}$, and $\dot{\theta}_k$ with respect to $w$, our final objective function $J_{\text{ESRA}} = J_{\text{ESRA}}^1 + J_{\text{ESRA}}^2$ is also linear in terms of $w$, allowing us to once again approach this problem using least squares. However, since we do not explicitly command the knee angle, we must enforce joint limits to ensure the Power Knee stays within its RoM, $\theta_k \in [0, 120]$, yielding a constrained least squares problem which can be solved using a Quadratic Program. The resultant kinematic surface is shown in Fig. 2 (right) for a fixed speed of 1 m/s. Fig. 3 shows the simulated foot trajectories for both models in comparison to reference data.

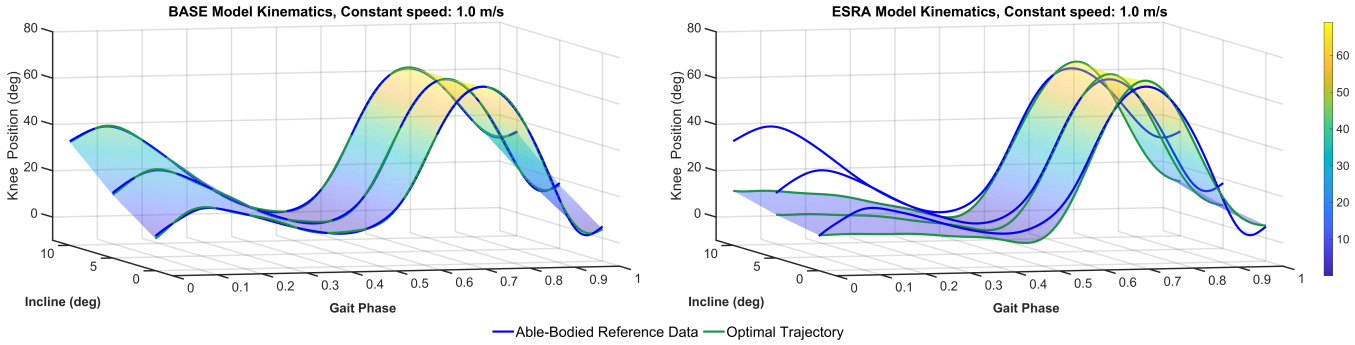


Fig. 2. Kinematic Surfaces for the baseline (BASE) and ESR-Adapted (ESRA) controllers for a constant walking speed of 1 m/s. Note the optimized and able-bodied reference trajectories from [37] overlap for the BASE controller but not for the ESRA controller.

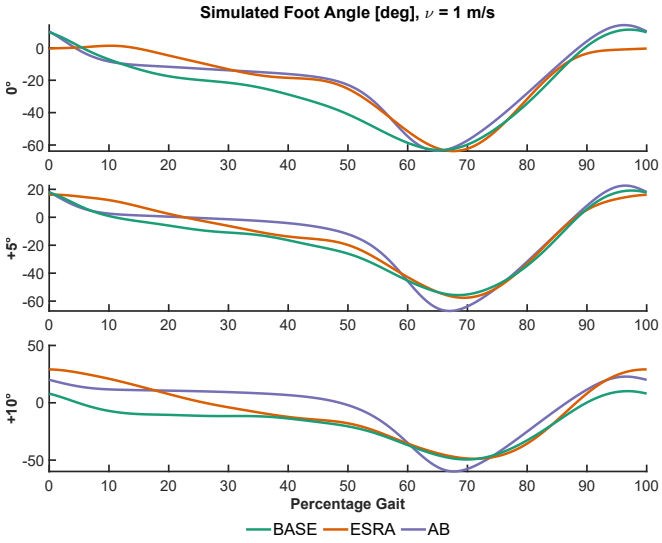


Fig. 3. Simulated optimal foot trajectories for the BASE and ESRA kinematic models, with Able-Bodied data (AB) as reference trajectories.

### D. Experiment Design

One pilot transfemoral amputee subject (male, 23 years, 80 kg with prosthesis, 175 cm, activity level K4) was enrolled in our study and provided written informed consent in accordance with the Institutional Review Board of the University of Michigan (HUM00230065). The subject wore a motion capture suit and was equipped with a set of motion capture markers on the legs and torso. For each controller, the subject walked on an instrumented treadmill (Bertec Corporation, Columbus, OH) at a fixed 1.0 m/s speed for three inclines (0, 5, 10 deg) for 150 seconds each. Before each trial, the Power Knee was configured to use the correct controller, and the correct parameter set corresponding to the current incline was manually selected. Although previous work has enabled real-time incline estimation using this control framework [22], we manually set the incline estimate in this preliminary work to isolate the effects of our modified kinematic model.

The instrumented split-belt treadmill collected ground reaction force (GRF) data for each leg at 1000 Hz. A motion capture system (Vicon, Oxford, UK) was used to record 3D positions of all markers at 250 Hz. The first 30 seconds of data for each trial were excluded from processing to restrict our analysis to steady-state walking. We processed the steady-state data in OpenSim 4.5 (Stanford, CA, USA) using the model from Rajagopal et al. [38] with modifications made to account for the Power Knee's inertial properties, similar to [39].

## III. Results

Figures 4 presents the average kinematic and GRF trajectories for each trial, along with reference able-bodied data. Table I presents normalized root mean square errors (NRMSE) for kinematics and GRF trajectories for each controller compared to able-bodied reference data, presented as a percentage of the range of each trajectory.

### A. Kinematics

On level ground, the two controllers behaved similarly, as shown by similar NRMSE values compared to able-bodied gait (Table I). This result was expected as the ESR foot's RoM is closer to that of normative ankle motion in level walking. In fact, experimental foot angle trajectories only differed slightly, with the BASE controlled foot briefly plantarflexing then dorsiflexing in midstance while the ESRA controlled foot remained planted (Fig. 4, column 1). This deviation grew to 10 deg of excess plantarflexion on steeper inclines (see supplementary video). The corrective behavior by the ESRA controller remained across all three inclines, as NRMSE in foot angle remained approximately the same for the ESRA controller whereas the BASE controller's NRMSE steadily increased with incline (Table I).

Due to differences in their optimization objectives, the controllers exhibited distinct knee trajectories when compared to able-bodied data. The BASE controller was able to retain a near-normative level of stance phase knee flexion, although the peak flexion occurred later in stance, perhaps due to the position controller gains not being strong enough to counteract the ESR foot's limited deflection. The ESRA controller, on the other hand, had stance-phase knee flexion peaks aligned in phase but not in magnitude: the prioritization of foot-angle tracking combined with the fixed-ankle assumption resulted in reduced peak knee flexion and earlier extension of the knee during stance phase (Fig. 4, column 2). At 10 deg, both kinematic models exhibited worsened performance due to ESR feet being unable to replicate the

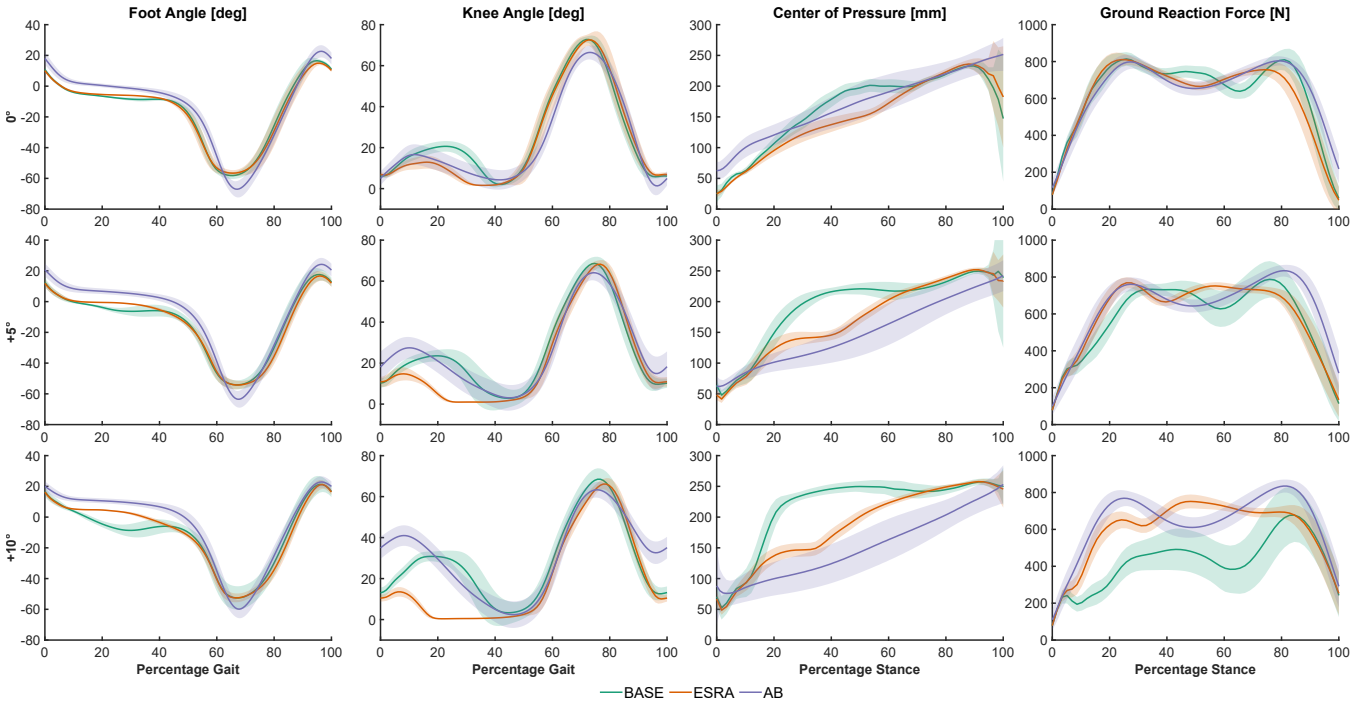


Fig. 4. Average experimental kinematic trajectories and ground reaction force data from both controllers. For able bodied reference data (AB) from [37], inter-subject averages are shown. Shaded regions represent $\pm 1$ standard deviation of data. Note for Center of Pressure and Ground Reaction Force, only stance phase is shown ($s \leq s_{\text{TO}}$).

TABLE I
NORMALIZED ROOT MEAN SQUARE ERROR ACROSS INCLINES

| | 1.0 m/s, 0° | | 1.0 m/s, +5° | | 1.0 m/s, +10° | |
|---|---|---|---|---|---|---|
| | BASE | ESRA | BASE | ESRA | BASE | ESRA |
| $\theta_{\text{foot}}$ (%) | 7.95 | 7.56 | 9.26 | 8.40 | 11.59 | 8.45 |
| $\theta_k$ (%) | 9.99 | 7.88 | 9.06 | 13.17 | 16.51 | 26.89 |
| CoP (%) | 25.96 | 19.80 | 23.40 | 11.70 | 29.72 | 16.38 |
| GRF (%) | 10.84 | 13.40 | 14.79 | 14.78 | 29.55 | 13.27 |

high biological ankle RoM observed at this incline. The reduced stance flexion commanded by the ESRA controller resulted in a substantial increase in knee angle NRMSE (13.17% at 5 deg and 26.89% at 10 deg) compared to the BASE controller, which has the sole objective of knee-angle tracking (9.06% at 5 deg and 16.51% at 10 deg). The periodicity requirement for the optimal trajectories resulted in these deviations from able-bodied gait in late swing phase, as the ESRA controller's heel strike target angle was substantially more extended than that of able-bodied data. We will see below that these deviations from able-bodied knee kinematics are a necessary tradeoff in pursuit of favorable ground contact with an ESR foot on inclines.

### B. Ground Interactions

The kinematics results discussed above help explain the causes for changes in ground interaction between the two position controllers. Incorrect placement of the ESR foot throughout stance phase by the BASE controller prevented proper loading of the device, while the ESRA controller's corrected positioning substantially improved prosthesis loading and resultant ground interactions. To analyze these changes, we first examined Center of Pressure (CoP), which we defined as the distance between the heel marker and the point at which the net GRF acts on the foot. As seen in the representative able-bodied trajectories in Fig. 4 (column 3), CoP should smoothly progress through stance phase as the foot rolls over from heel to toe.

The BASE controller did not produce the smooth CoP progression we would expect and instead underwent rapid progression for the first half of stance phase (Fig. 4, column 3). On level ground, the prosthesis geometry allowed the heel to still take the majority of the user's weight, but on steeper inclines, this resulted in forefoot strikes rather than heel strikes. As a result, the foot visibly bounced as the keel unloaded in midstance, where the CoP regressed slightly and lost monotonicity. This trend can be seen through the NRMSE for CoP (Table I), for which the BASE values are substantially higher than those of the ESRA controller across inclines.

The ESRA controller significantly mitigated, but did not completely remove, this rapid progression. Proper foot placement allowed the heel to be loaded, delaying initial rollover making for a smoother stance phase progression. This loading on the ESRA controller was similar in magnitude to able-bodied GRF data, whereas the BASE controlled prosthesis was far under-loaded on steeper inclines (Fig. 4, column 4). While the ESRA controller allowed the user to properly bear weight with their prosthesis throughout stance phase, the loading profile still departed from the standard "M-shape" seen in able-bodied reference data. This trend was most noticeable at 10 deg, where the heel of the prosthesis could not be sufficiently loaded while using the BASE controller.

The user's confidence in the prosthesis lowered due to the resulting irregular foot behavior, leading to lower weight bearing and GRF throughout stance phase, as shown in Fig. 4 (Row 3, Column 4). The NRMSE compared to reference GRF data was 29.55% for the BASE controller and 13.27% for the ESRA controller (Table I).

## IV. Discussion

By attempting to follow able-bodied trajectories at the knee, the BASE controller implicitly expects biological ankle behavior from the ESR foot. As the ESR foot cannot fully exhibit normative ranges of motion across steeper inclines, the foot is incorrectly loaded through stance phase, leading to departures from normative kinematics and kinetics. The ESRA controller is able to mitigate these issues rather well, even if the controller cannot completely return the prosthesis to able-bodied behavior.

Another observation is that these notable improvements from the ESRA controller are not a result of increased RoM, but rather shifting foot placement. The model for finding optimal trajectories, along with the controller itself, have no knowledge about the ESR foot or how it will behave: the performance changes emerge solely from the foot landing in a more favorable configuration which can better absorb and return energy through stance phase.

Ultimately, able-bodied gait may not be a proper objective choice for powered-knee, passive-ankle prostheses, since prostheses with ESR feet cannot perfectly replicate able-bodied movement in all tasks. Rather, perhaps a more fitting target for kinematics and kinetics is data from transtibial amputees, whose intact biological knees optimally adjust to using ESR feet. Future work for powered-knee, passive-ankle prostheses could incorporate transtibial amputee gait data for a more achievable reference trajectory set, although a dataset with sufficient data across a range of activities would need to be collected to enable this approach.

### A. Limitations

The modeling assumption of a fixed ankle joint is a strong simplification which directly affects the extent of differences between the BASE and ESRA models. This is evident from the large deviations between the simulated (Fig. 3) and experimental (Fig. 4) foot trajectories, as the ESR foot bends enough such that the prosthesis is always more plantarflexed than representative able-bodied data. A foot-deflection model which relates GRF to ankle angle would allow for the limited ankle RoM of ESR feet to be taken into account, although the wide variety of ESR feet would make it difficult to generalize these results. If a generalized ESR foot deflection model could be developed, this would result in less extreme adjustments to knee trajectories for the ESRA controller.

Further, the incline setting in the controller was manually configured by a researcher in these experiments. Outside of the laboratory environment, we aim for these devices to automatically discern inclines as the user walks to allow for seamless adaptation between slopes. Future work will involve collecting data from the device's sensing suite in order to correlate existing signals with the current ground slope. While an additional, foot-mounted IMU sensor could trivialize this task, maintaining the existing sensor set on the Power Knee would be preferable for rapid translation of our control methods to clinical use.

Finally, the results in this work come from a pilot study with a single participant who had familiarity with the controller implemented on the Power Knee. As such, we are unable to generalize any claims about the trends and results observed. We intend to run a validation study with more participants in future work, which will also consider additional terrains such as declined ramps and uneven outdoor surfaces.

## V. Conclusion

By indirectly controlling foot angle, as opposed to directly controlling the knee angle, the proposed control method allows for improved ground-contact behavior and proper loading of the ESR foot in a powered-knee, passive-ankle prosthesis. The effect is particularly evident while navigating steeper inclines. In a pilot subject experiment, our proposed controller results in substantial improvements in kinematics and ground interactions, showing that biomimicry can remain a feasible objective despite ESR feet's limited ability to mimic a biological ankle. This work serves as a step towards translation of versatile, biomimetic control methods from the research field onto commercially available clinical hardware, strengthening the case for widespread adoption of powered prostheses.


## ACKNOWLEDGMENTS

The authors would like to thank Atli Örn Sverrisson and David Langlois for assistance with the Power Knee hardware and Jeffrey Wensman, CPO for clinical support.


## Competing Interest Disclosures

The authors are listed on patents or patent applications related to the HKIC control method.

Hardware and related support was provided by Össur hf (Reykjavík, Iceland), which could have a financial interest in the results of this study. The results and conclusions in this work are entirely those of the authors and may not reflect the views of Össur hf or the National Institutes of Health.

## References


[1] M. Caruso and S. Harrington, "Prevalence of Limb Loss and Limb Difference in the United States: Implications for Public Policy," 2024.

[2] J. A. Rivera, K. Churovich, A. B. Anderson, and B. K. Potter, "Estimating Recent US Limb Loss Prevalence and Updating Future Projections," *Archives of Rehabilitation Research and Clinical Translation*, p. 100376, Oct. 2024.

[3] R. L. Waters, J. Perry, D. Antonelli, and H. Hislop, "Energy cost of walking of amputees: the influence of level of amputation," *The Journal of Bone and Joint Surgery. American Volume*, vol. 58, no. 1, pp. 42–46, Jan. 1976.

[4] A. S. Göktepe, B. Cakir, B. Yilmaz, and K. Yazicioglu, "Energy expenditure of walking with prostheses: comparison of three amputation levels," *Prosthetics and Orthotics International*, vol. 34, no. 1, pp. 31–36, Mar. 2010.

[5] R. Gehlhar, M. Tucker, A. J. Young, and A. D. Ames, "A review of current state-of-the-art control methods for lower-limb powered prostheses," *Annual Reviews in Control*, vol. 55, pp. 142–164, Jan. 2023.

[6] S. K. Au, J. Weber, and H. Herr, "Powered Ankle–Foot Prosthesis Improves Walking Metabolic Economy," *IEEE Trans. Robotics*, vol. 25, no. 1, pp. 51–66, Feb. 2009.

[7] E. C. Martinez-Villalpando, L. Mooney, G. Elliott, and H. Herr, "Antagonistic active knee prosthesis. A metabolic cost of walking comparison with a variable-damping prosthetic knee," in *Annu. Int. Conf. of the IEEE Eng. in Med. and Biol. Soc.*, vol. 2011, 2011, pp. 8519–8522.

[8] E. D. Ledoux and M. Goldfarb, "Control and Evaluation of a Powered Transfemoral Prosthesis for Stair Ascent," *IEEE Trans Neural Syst Rehabil Eng*, vol. 25, no. 7, pp. 917–924, Jul. 2017.

[9] A. M. Simon, K. A. Ingraham, N. P. Fey, S. B. Finucane, R. D. Lipschutz, A. J. Young, and L. J. Hargrove, "Configuring a Powered Knee and Ankle Prosthesis for Transfemoral Amputees within Five Specific Ambulation Modes," *PLOS ONE*, vol. 9, no. 6, p. e99387, Jun. 2014, publisher: Public Library of Science.

[10] C. L. Brockett and G. J. Chapman, "Biomechanics of the ankle," *Orthop Trauma*, vol. 30, no. 3, p. 232, Jun. 2016.

[11] A. S. McIntosh, K. T. Beatty, L. N. Dwan, and D. R. Vickers, "Gait dynamics on an inclined walkway," *J. Biomechanics*, vol. 39, no. 13, pp. 2491–2502, Jan. 2006.

[12] N. T. Pickle, A. M. Grabowski, J. R. Jeffers, and A. K. Silverman, "The Functional Roles of Muscles, Passive Prostheses, and Powered Prostheses During Sloped Walking in People With a Transtibial Amputation," *J. Biomechanical Eng.*, vol. 139, no. 111005, Oct. 2017.

[13] F. B. Rodrigues, G. S. de Sá e Souza, E. de Mendonça Mesquita, R. de Sousa Gomide, R. R. Baptista, A. A. Pereira, A. O. Andrade, and M. F. Vieira, "Margins of stability of persons with transtibial or transfemoral amputations walking on sloped surfaces," *J. Biomechanics*, vol. 123, p. 110453, Jun. 2021.

[14] N. T. Pickle, J. M. Wilken, J. M. Aldridge Whitehead, and A. K. Silverman, "Whole-body angular momentum during sloped walking using passive and powered lower-limb prostheses," *Journal of Biomechanics*, vol. 49, no. 14, pp. 3397–3406, Oct. 2016.

[15] A. H. Vrieling, H. G. van Keeken, T. Schoppen, E. Otten, J. P. K. Halbertsma, A. L. Hof, and K. Postema, "Uphill and downhill walking in unilateral lower limb amputees," *Gait & Posture*, vol. 28, no. 2, pp. 235–242, Aug. 2008.

[16] D. C. Morgenroth, M. Roland, A. L. Pruziner, and J. M. Czerniecki, "Transfemoral amputee intact limb loading and compensatory gait mechanics during down slope ambulation and the effect of prosthetic knee mechanisms," *Clin. Biomechanics*, vol. 55, pp. 65–72, Jun. 2018, publisher: Elsevier.

[17] T. Schmalz, S. Blumentritt, and B. Marx, "Biomechanical analysis of stair ambulation in lower limb amputees," *Gait & Posture*, vol. 25, no. 2, pp. 267–278, Feb. 2007.

[18] W. L. Childers and K. Z. Takahashi, "Increasing prosthetic foot energy return affects whole-body mechanics during walking on level ground and slopes," *Scientific Reports*, vol. 8, no. 1, p. 5354, Mar. 2018.

[19] N. P. Fey, G. K. Klute, and R. R. Neptune, "The influence of energy storage and return foot stiffness on walking mechanics and muscle activity in below-knee amputees," *Clinical Biomechanics*, vol. 26, no. 10, pp. 1025–1032, Dec. 2011.

[20] B. J. Hafner, J. E. Sanders, J. Czerniecki, and J. Fergason, "Energy storage and return prostheses: does patient perception correlate with biomechanical analysis?" *Clin. Biomechanics*, vol. 17, no. 5, pp. 325–344, Jun. 2002.

[21] D. Quintero, D. J. Villarreal, D. J. Lambert, S. Kapp, and R. D. Gregg, "Continuous-Phase Control of a Powered Knee–Ankle Prosthesis: Amputee Experiments Across Speeds and Inclines," *IEEE Trans. Robotics*, vol. 34, no. 3, pp. 686–701, Jun. 2018.

[22] T. K. Best, C. G. Welker, E. J. Rouse, and R. D. Gregg, "Data-Driven Variable Impedance Control of a Powered Knee–Ankle Prosthesis for Adaptive Speed and Incline Walking," *IEEE Trans. Robotics*, vol. 39, no. 3, pp. 2151–2169, Jun. 2023.

[23] L. M. Sullivan, S. Creveling, M. Cowan, L. Gabert, and T. Lenzi, "Powered Knee and Ankle Prosthesis Control for Adaptive Ambulation at Variable Speeds, Inclines, and Uneven Terrains," *IEEE/RSJ Int. Conf. on Intell. Robot. and Syst.*, vol. 2023, pp. 2128–2133, Oct. 2023.

[24] R. J. Cortino, T. K. Best, and R. D. Gregg, "Data-Driven Phase-Based Control of a Powered Knee-Ankle Prosthesis for Variable-Incline Stair Ascent and Descent," *IEEE Trans. on Med. Robot. and Bionics*, vol. 6, no. 1, pp. 175–188, Feb. 2024.

[25] S. Hood, L. Gabert, and T. Lenzi, "Powered Knee and Ankle Prosthesis With Adaptive Control Enables Climbing Stairs With Different Stair Heights, Cadences, and Gait Patterns," *IEEE Trans. Robotics*, vol. 38, no. 3, pp. 1430–1441, Jun. 2022.

[26] S. Cheng, C. A. Laubscher, and R. D. Gregg, "Controlling Powered Prosthesis Kinematics Over Continuous Inter-Leg Transitions Between Walking and Stair Ascent/Descent," *IEEE Trans. Neural Syst. and Rehabil. Eng.*, vol. 32, pp. 3891–3901, 2024.

[27] M. A. Holgate, T. G. Sugar, and A. W. Bohler, "A novel control algorithm for wearable robotics using phase plane invariants," in *2009 IEEE Int. Conf. on Robot. and Automat.*, May 2009, pp. 3845–3850, iSSN: 1050-4729.

[28] R. D. Gregg, T. Lenzi, L. J. Hargrove, and J. W. Sensinger, "Virtual Constraint Control of a Powered Prosthetic Leg: From Simulation to Experiments with Transfemoral Amputees," *IEEE Trans. Robotics*, vol. 30, no. 6, p. 1455, Dec. 2014.

[29] N. Thatte, T. Shah, and H. Geyer, "Robust and Adaptive Lower Limb Prosthesis Stance Control via Extended Kalman Filter-Based Gait Phase Estimation," *IEEE Robotics and Automation Letters*, vol. 4, no. 4, pp. 3129–3136, Oct. 2019.

[30] S. Rezazadeh, D. Quintero, N. Divekar, E. Reznick, L. Gray, and R. D. Gregg, "A Phase Variable Approach for Improved Rhythmic and Non-Rhythmic Control of a Powered Knee-Ankle Prosthesis," *IEEE access: practical innovations, open solutions*, vol. 7, pp. 109 840–109 855, 2019.

[31] K. R. Embry, D. J. Villarreal, R. L. Macaluso, and R. D. Gregg, "Modeling the Kinematics of Human Locomotion Over Continuously Varying Speeds and Inclines," *IEEE Trans. Neural Syst. and Rehabil. Eng.*, vol. 26, no. 12, pp. 2342–2350, Dec. 2018.

[32] T. K. Best, K. R. Embry, E. J. Rouse, and R. D. Gregg, "Phase-Variable Control of a Powered Knee-Ankle Prosthesis over Continuously Varying Speeds and Inclines," in *2021 IEEE/RSJ Int. Conf. Intell. Robot. and Syst. (IROS)*, Sep. 2021, pp. 6182–6189, iSSN: 2153-0866.

[33] C. G. Welker, T. K. Best, and R. D. Gregg, "Improving Sit/Stand Loading Symmetry and Timing Through Unified Variable Impedance Control of a Powered Knee-Ankle Prosthesis," *IEEE Trans. Neural Syst. and Rehabil. Eng.*, vol. 31, pp. 4146–4155, 2023.

[34] T. K. Best, C. A. Laubscher, R. J. Cortino, S. Cheng, and R. D. Gregg, "Improving Amputee Endurance Over Activities of Daily Living with a Robotic Knee-Ankle Prosthesis: A Case Study," in *2023 IEEE/RSJ Int. Conf. Intell. Rob. and Syst. (IROS)*, Oct. 2023, pp. 2101–2107, iSSN: 2153-0866.

[35] T. Elery, S. Rezazadeh, C. Nesler, and R. D. Gregg, "Design and Validation of a Powered Knee–Ankle Prosthesis With High-Torque, Low-Impedance Actuators," *IEEE Trans. Robotics*, vol. 36, no. 6, pp. 1649–1668, Dec. 2020.

[36] S. Gudjonsson, A. Einarsson, H. I. Thorsteinsdottir, and D. Langlois, "Ground contact sensor array for lower-limb prosthetic and orthotic devices," US Patent 20 220 401 236A1, Dec., 2022.

[37] E. Reznick, K. R. Embry, R. Neuman, E. Bolívar-Nieto, N. P. Fey, and R. D. Gregg, "Lower-limb kinematics and kinetics during continuously varying human locomotion," *Scientific Data*, vol. 8, no. 1, p. 282, Oct. 2021.

[38] A. Rajagopal, C. L. Dembia, M. S. DeMers, D. D. Delp, J. L. Hicks, and S. L. Delp, "Full-Body Musculoskeletal Model for Muscle-Driven Simulation of Human Gait," *IEEE transactions on bio-medical engineering*, vol. 63, no. 10, pp. 2068–2079, Oct. 2016.

[39] V. Raveendranathan, V. G. M. Kooiman, and R. Carloni, "Musculoskeletal model of osseointegrated transfemoral amputees in OpenSim," *PloS One*, vol. 18, no. 9, p. e0288864, 2023.